

Article

An AlGa_N/Ga_N Lateral Bidirectional Current-Regulating Diode with Two Symmetrical Hybrid Ohmic-Schottky Structures

Yijun Shi , Zongqi Cai ^{*}, Yun Huang, Zhiyuan He ^{*}, Yiqiang Chen , Liye Cheng and Guoguang Lu

National Key Laboratory of Science and Technology on Reliability Physics and Application of Electronic Component, China Electronic Product Reliability and Environmental Testing Research Institute, Guangzhou 510610, China; syj20094870@sina.com (Y.S.); huangyun@ceppei.com (Y.H.); yiqiang-chen@hotmail.com (Y.C.); q1238199@163.com (L.C.); luguoguang@ceppei.com (G.L.)
^{*} Correspondence: zqcai.uestc@hotmail.com (Z.C.); hezhizhuan1988@126.com (Z.H.); Tel.: +86-18565592910 (Z.H.)

Abstract: Bidirectional current-regulating ability is needed for AC light emitting diode (LED) drivers. In previous studies, various rectifier circuits have been used to provide constant bidirectional current. However, the usage of multiple electronic components can lead to additional costs and power consumption. In this work, a novel AlGa_N/Ga_N lateral bidirectional current-regulating diode (B-CRD) featuring two symmetrical hybrid-trench electrodes is proposed and demonstrated by TCAD Sentaurus (California USA) from Synopsys corporation. Through shortly connecting the Ohmic contact and trench Schottky contact, the unidirectional invariant current can be obtained even with the applied voltage spanning a large range of 0–200 V. Furthermore, with the combination of two symmetrical hybrid-trench electrodes at each side of the device, the proposed B-CRD can deliver an excellent steady current in different directions. Through the TCAD simulation results, it was found that the device's critical characteristics (namely knee voltage and current density) can be flexibly modulated by tailoring the depth and length of the trench Schottky contact. Meanwhile, it was also demonstrated through the device/circuit mixed-mode simulation that the proposed B-CRD can respond to the change in voltage in a few nanoseconds. Such a new functionality combined with excellent performance may make the proposed B-CRD attractive in some special fields where the bidirectional current-limiting function is needed.

Keywords: current-regulating diode; hybrid-trench electrode; AlGa_N/Ga_N; B-CRD



Citation: Shi, Y.; Cai, Z.; Huang, Y.; He, Z.; Chen, Y.; Cheng, L.; Lu, G. An AlGa_N/Ga_N Lateral Bidirectional Current-Regulating Diode with Two Symmetrical Hybrid Ohmic-Schottky Structures. *Micromachines* **2022**, *13*, 1157. <https://doi.org/10.3390/mi13071157>

Academic Editors: Alessandro Chini, Nicolo Zagni and Niall Tait

Received: 17 June 2022

Accepted: 19 July 2022

Published: 21 July 2022

Publisher's Note: MDPI stays neutral with regard to jurisdictional claims in published maps and institutional affiliations.



Copyright: © 2022 by the authors. Licensee MDPI, Basel, Switzerland. This article is an open access article distributed under the terms and conditions of the Creative Commons Attribution (CC BY) license (<https://creativecommons.org/licenses/by/4.0/>).

1. Introduction

As a representative of wide-bandgap semiconductors, gallium nitride (Ga_N) has attracted increasing interest in high-voltage and high-power applications, due to its high critical electric field strength, high electron mobility, high saturation electron drift velocity, and high thermal conductivity [1]. The AlGa_N/Ga_N high electron mobility transistor (HEMT) and metal-insulator-semiconductor HEMT (MIS-HEMT) are the most studied Ga_N-based power transistors, due to their high breakdown voltage, high switching frequency, low specific on-resistance, and especially the polarization-induced high-mobility and high-density two-dimensional electron gases (2DEG) within the AlGa_N/Ga_N heterointerface [2]. Meanwhile, two-terminal power electronics are also indispensable components in a power electronic system, such as AlGa_N/Ga_N lateral Schottky barrier diodes [3], AlGa_N/Ga_N lateral field-effect rectifiers [4] and current-regulating diodes (CRD) [5,6]. Similar to the constant-current source based on integrated circuits, CRDs capable of providing a unidirectional invariant current are widely used in many power electronic systems, such as light emitting diode (LED) lighting systems and current-source systems for piezoelectric actuators.

Traditional circuits used to drive LEDs can be divided into switching constant-current modes and linear constant-current modes [7–9], which compose of multiple devices. In a

typical linear constant-current driver circuit for an LED, N-Metal-Oxide-Semiconductor (NMOS), as the main power device, is connected in series with the LED and works in the linear amplification region. Additionally, the driving current of the LED can be adjusted by changing the gate voltage of NMOS. Another typical linear driver circuit for LEDs is the mirror constant-current circuit. The main power device, NMOS, also works in the linear amplification region. In this way, the current generated by the constant-current circuit will flow through the mirror circuit composed of two power devices to transfer a stable current to the LED, so that the driving current for the LED remains unchanged. In the application of medium- and small-power situations, a linear constant-current driver circuit has a low cost, a simple structure, a high efficiency, a small volume and low electromagnetic interference. It is also very suitable for indoor LED lamps (such as LED fluorescent lamps). However, a linear constant-current driver circuit is less used in high-power situations because of its low efficiency [10]. Different from the linear constant-current mode, power devices in switching constant-current circuits work in a high-speed switching state, which is controlled by switching power supply technology, so that the circuit can have a constant output current. However, a switching constant-current circuit is complex and requires a large board size. Based on the working characteristics of LEDs and the development trend of miniaturization in the semiconductor industry, LED driver circuits will be designed in a more simplified direction, and LED constant-current driver ICs will be more integrated. Constant-current driver circuits composed of CRDs are becoming more and more popular in the market. Compared with constant-current sources based on integrated circuits, CRDs are preferred due to their simple structure, high reliability, and strong anti-interference ability. In addition, they can protect LEDs from damage caused by a change in over-current, over-voltage and cycle number.

Although AlGaIn/GaN CRDs are scarcely reported, developing a high-performance power electronic system based on AlGaIn/GaN CRDs is of great potential. For example, high-performance single-chip LED lighting systems could be achieved through monolithically integrating AlGaIn/GaN CRDs with GaN-based LEDs [11,12]. Furthermore, owing to their wide bandgap, AlGaIn/GaN CRDs are also preferred for battery charge/discharge in harsh environments. We have proposed and experimentally investigated an AlGaIn/GaN CRD based on a single hybrid Ohmic-Schottky structure [13]. Through shortly connecting the Ohmic contact and trench Schottky contact, the invariant current could be obtained for the proposed AlGaIn/GaN CRD even with an applied voltage spanning a large range of 0–200 V and a wide temperature range from $-50\text{ }^{\circ}\text{C}$ to $250\text{ }^{\circ}\text{C}$. Meanwhile, the proposed AlGaIn/GaN CRD exhibited a fast response capability. However, the proposed AlGaIn/GaN CRD was only capable of providing an invariant current in one direction, and cannot provide an invariant current in another direction. CRDs with the capability of providing bidirectional invariant current is also needed in some application fields, such as AC LED lighting systems, battery charging/discharging systems, solar photovoltaic power generation systems, and energy management systems of electric vehicles [14,15]. In previous studies, various rectifier circuits have been to provide bidirectional constant current [16–18]. However, the usage of multiple electronic components can lead to additional costs and power consumption.

In this work, a novel AlGaIn/GaN lateral bidirectional current-regulating diode (B-CRD) is proposed and demonstrated by TCAD Sentaurus. With the combination of two symmetrical hybrid-trench electrodes at each side of the device, the proposed B-CRD could deliver an excellent steady current in different directions. Furthermore, for the case of saving manpower, material resources, and time costs, the TCAD simulation was employed to investigate the proposed AlGaIn/GaN B-CRD. The manuscript is organized as follows: the structure and mechanism of the proposed AlGaIn/GaN B-CRD are briefly introduced in Part II; the device's characteristics and their dependence on the thickness and length of AlGaIn under the trench Schottky contact region (T_{AlGaIn} and L_G) are investigated in Part III; the conclusion is given in Part IV.

2. Structure and Mechanism

Figure 1 shows the schematic cross-section and equivalent circuit of the proposed AlGa_N/Ga_N lateral B-CRD, which features two symmetrical hybrid-trench electrodes at each side of the device (Figure 1a). Both hybrid-trench electrodes consisted of a recessed Schottky contact structure and an Ohmic contact structure (Sch-A/C and Ohm-A/C, the left electrode is defined as the anode, the right electrode is defined as the cathode). The short connection of the recessed Schottky contact structure and Ohmic contact structure was able to provide an invariant current even with the applied voltage spanning a large range of 0–200 V. So, every hybrid-trench electrode could be treated as a unidirectional AlGa_N/Ga_N lateral CRD, just as the experiment results in our previous work demonstrate [13]. The equivalent circuit of the unidirectional AlGa_N/Ga_N lateral CRD is drawn under the recessed Schottky-contact structure (Figure 1a). For the proposed AlGa_N/Ga_N lateral B-CRD, the hybrid-trench electrode at each side of the device could be regarded as a unidirectional AlGa_N/Ga_N lateral CRD (Figure 1b). With the anti-series connection of two unidirectional CRDs, the proposed AlGa_N/Ga_N lateral B-CRD was able to deliver an excellent steady current in different directions. The detailed working mechanism of the proposed AlGa_N/Ga_N lateral B-CRD is explained in Figures 2 and 3.

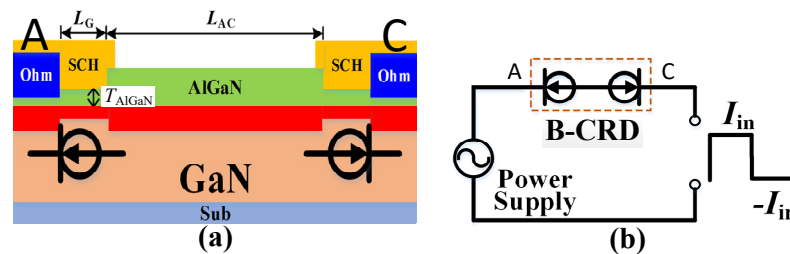


Figure 1. Schematic cross-section (a) and equivalent circuit (b) of the proposed AlGa_N/Ga_N lateral B-CRD with two symmetrical hybrid-trench electrodes at each side of the device.

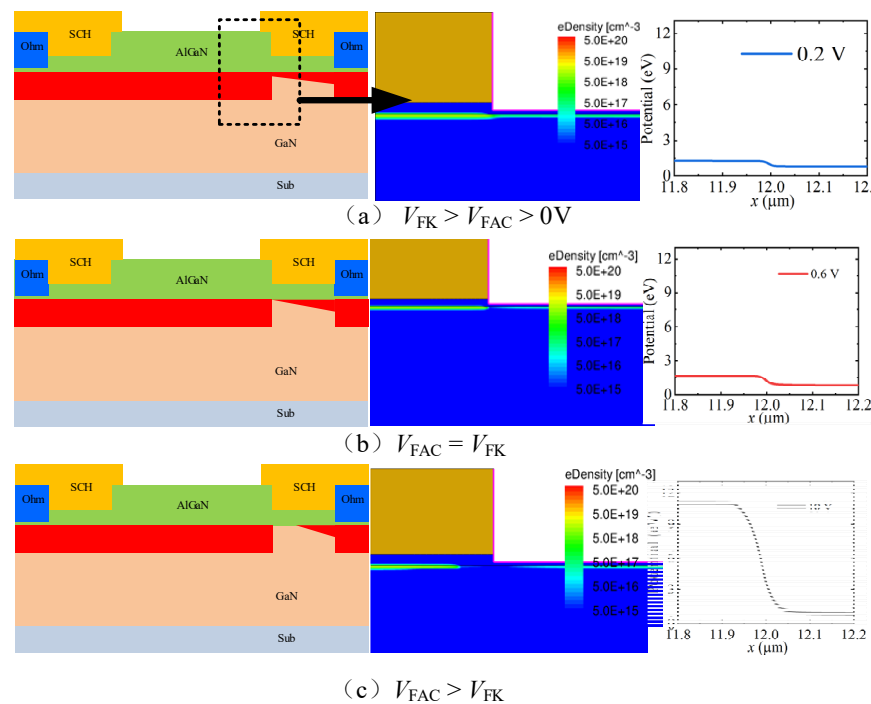


Figure 2. The forward working mechanism of the proposed AlGa_N/Ga_N lateral B-CRD: (a) $V_{FK} > V_{FAC} > 0$ V; (b) $V_{FAC} = V_{FK}$; (c) $V_{FAC} > V_{FK}$.

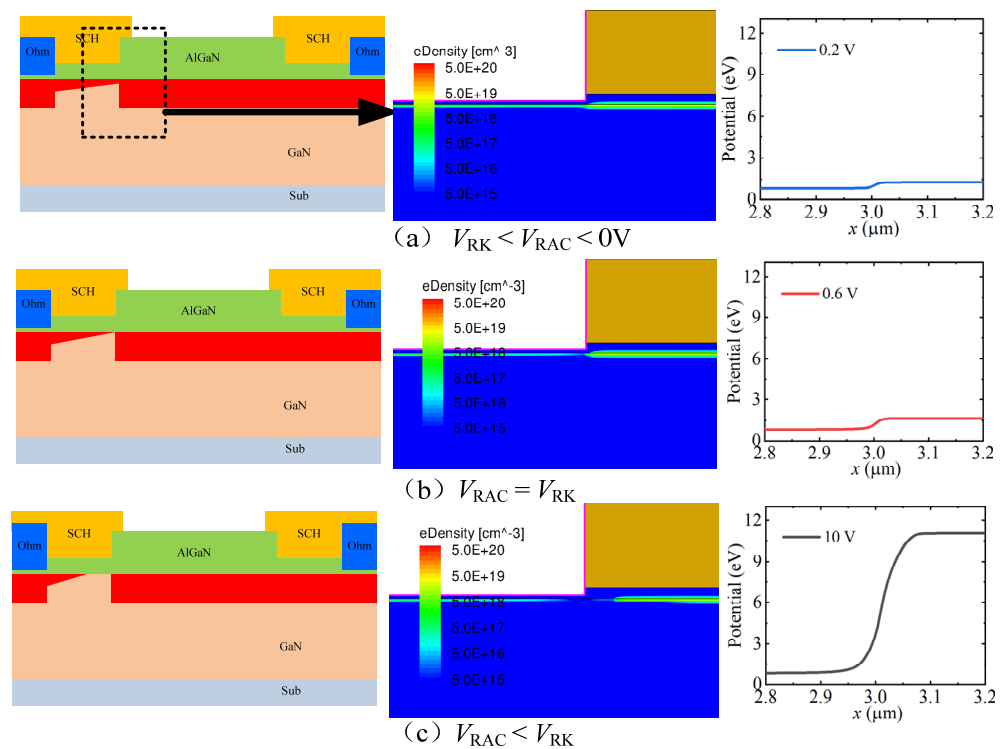


Figure 3. The reverse working mechanism of the proposed AlGaIn/GaN lateral B-CRD: (a) $V_{FK} > V_{FAC} > 0\text{ V}$; (b) $V_{FAC} = V_{FK}$; (c) $V_{FAC} > V_{FK}$.

In the forward conduction state, the voltage drop was concentrated under the Sch-C region, which depleted the 2DEG under the Sch-C region, as shown in Figure 2. When the forward anode-to-cathode voltage (V_{FAC}) was less than the forward-knee voltage (V_{FK}), there was still a lot of two-dimensional electron gas (2DEG) under the Sch-C region, as shown in Figure 2a. In this stage, the forward anode-to-cathode current increased with the increase in the forward anode-to-cathode voltage, which also lead the 2DEG under the Sch-C region to be gradually depleted. When the forward anode-to-cathode voltage was equal to the forward knee voltage, the 2DEG channel was pinched off at the left side of the Sch-C region (as shown in Figure 2b), and a further increase in the forward anode-to-cathode voltage lead to the depletion area moving under the Sch-C region (as shown in Figure 2c). At this moment, the forward anode-to-cathode current did not continue to be increased with an increase in the forward anode-to-cathode voltage. The forward knee voltage and the forward constant-current density as the critical characteristics of the proposed AlGaIn/GaN lateral B-CRD were determined by the depth and length of the trench Sch-C region. With the recessed Sch-C structure embedded into the AlGaIn barrier layer, the depletion region under the recessed Schottky contact structure could be formed under a very low forward anode-to-cathode voltage, enabling the forward anode-to-cathode current density to become constant quickly.

The same thing happened in the reverse conduction state. In the reverse conduction state, the voltage drop was concentrated under the Sch-A region, which lead to the depletion of the 2DEG under the Sch-A region, as shown in Figure 3. When the reverse anode-to-cathode voltage (V_{RAC}) was less than the reverse knee voltage (V_{RK}), the reverse anode-to-cathode current increased with an increase in the reverse anode-to-cathode voltage, due to there still being a lot of 2DEG under the Sch-A region, as shown in Figure 3a. When the reverse anode-to-cathode voltage was equal to the reverse knee voltage, the 2DEG channel was pinched off at the right side of the Sch-A region (as shown in Figure 3b). With a further increase in the reverse anode-to-cathode voltage, the depletion area moved under the Sch-A region (as shown in Figure 3c), and the reverse anode-to-cathode current did not continue to be increased. The reverse knee voltage and the reverse constant-current

density were determined by the depth and length of the trench Sch-A region. With the recessed Sch-A structure embedded into the AlGa_N barrier layer, the depletion region under the recessed Schottky contact structure could be formed under a very low reverse anode-to-cathode voltage.

In this work, TCAD Sentaurus was used to investigate the characteristics of the proposed AlGa_N/Ga_N lateral B-CRD. The main physical models used in the simulation included a polarization model, an impact ionization model, and a high-field velocity saturation model [19–21]. The specific description of these models can be found in [21]. The correctness of the physical models employed in the simulation has been preliminarily verified in our previous work [19]. Furthermore, the experimental results in our previous work [13] were further used to correct the physical models employed in the simulation. The heterostructure employed in this work consisted of a 2 nm Ga_N cap, 23 nm Al_{0.23}Ga_{0.77}N barrier, 1 nm AlN spacer, and 3.5 μm Ga_N buffer, which was same as the heterostructure in our previous work [13]. In addition, the deep acceptor traps and self-compensating donor traps were also considered in the Ga_N buffer layer, with activation energies of $E_V + 0.9$ eV and $E_C - 0.11$ eV, and the trap densities were 3×10^{16} cm⁻³ and 1.3×10^{15} cm⁻³, respectively. Additionally, the unintentional doping concentration was set to be 1×10^{15} cm⁻³. The donor traps in the Nitride/Ga_N cap were considered with an activation energy of $E_C - 0.4$ eV and a density of 3×10^{13} cm⁻². In the beginning, the simulation results for the AlGa_N/Ga_N lateral CRD with $T_{\text{AlGa}_N} = 9$ nm and $L_G = 1$ μm were used to fit the experimental results to prove the correctness of the simulation. Then, the dependence of the proposed AlGa_N/Ga_N lateral B-CRD's characteristics on the depth and length of the trench Schottky contact were investigated. Finally, the device/circuit mixed-mode simulation was conducted to obtain the switching characteristics of the proposed AlGa_N/Ga_N lateral B-CRD.

3. Results and Discussion

3.1. Static Characteristics of the Proposed AlGa_N/Ga_N Lateral B-CRD

Figure 4 shows the simulated current-voltage (I - V) and breakdown voltage (BV) characteristics of the AlGa_N/Ga_N lateral CRD with $L_G = 1$ μm and $T_{\text{AlGa}_N} = 9$ nm, as well as our pervious experimental results in [13]. It can be seen from the figure, there was no significant difference between the simulated characteristics of the AlGa_N/Ga_N lateral CRD and the experimental results, which proves the correctness of the physical models employed in this research. In the following simulation work, the same physical models were employed to investigate the characteristics of the proposed AlGa_N/Ga_N lateral B-CRD and their dependence on the depth and length of the trench Schottky contact.

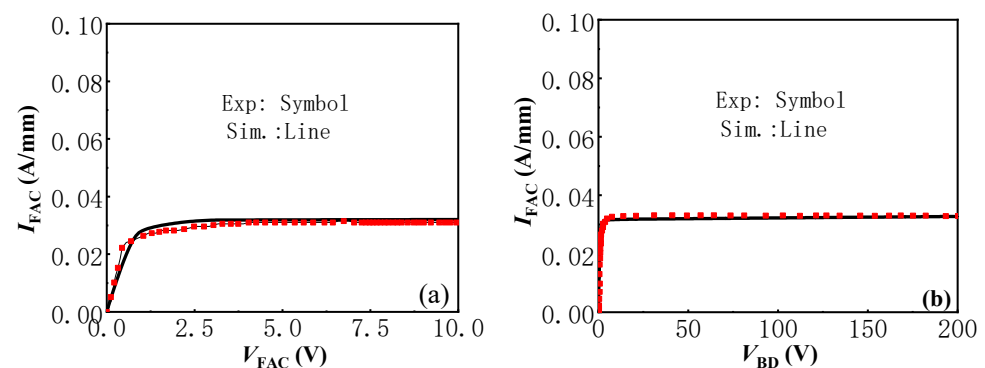


Figure 4. The I - V (a) and BV (b) characteristics of the AlGa_N/Ga_N lateral CRD with $L_G = 1$ μm and $T_{\text{AlGa}_N} = 9$ nm. Our pervious experimental results of the AlGa_N/Ga_N lateral CRD in [13] are also presented for comparison.

Figure 5 exhibits the simulated bidirectional I - V and BV characteristics of the proposed AlGa_N/Ga_N lateral B-CRD with $L_G = 1$ μm and $T_{\text{AlGa}_N} = 9$ nm, as well as the simulated

I - V and BV characteristics of the bidirectional diode without the Schottky electrode in the recessed structure. As stated above, the proposed AlGaIn/GaN lateral B-CRD was able to deliver an excellent steady current in not only the forward conduction state, but also the reverse conduction state. Furthermore, compared with the CRD in [5,6], the proposed AlGaIn/GaN lateral B-CRD delivered a steadier current even with the applied voltage spanning a large range of 0–200 V. Additionally, the knee voltage of the proposed AlGaIn/GaN lateral B-CRD was about 0.6 V, which was much lower than that of the CRD in [5,6] (about 3 V). Such a new functionality combined with the excellent performance may make the proposed AlGaIn/GaN lateral B-CRD attractive in some special fields, where a bidirectional current-limiting function is needed. In Figure 4, it was also found that the bidirectional diode without the Schottky electrode in the recessed structure could not deliver an invariant current with the applied voltage spanning a range of 0–200 V, which demonstrates that the Schottky contact electrode in the recessed structure played an important role in delivering an excellent steady current for the proposed AlGaIn/GaN lateral B-CRD. The influence of the temperature on the I - V characteristics of the proposed AlGaIn/GaN lateral B-CRD was also investigated, as shown in Figure 6. It can be seen that the current of the proposed AlGaIn/GaN lateral B-CRD decreased with an increase in temperature, which was due to the decrease in electron mobility. As the temperature increased from 25 °C to 225 °C, the current of the proposed AlGaIn/GaN lateral B-CRD decreased from 32 mA to 22 mA, a decrease of about 30%. However, it can be seen that the increase in the temperature had nearly no effect on the knee voltages of the proposed AlGaIn/GaN lateral B-CRD. The highly stable knee voltages may make the proposed AlGaIn/GaN lateral B-CRD more attractive.

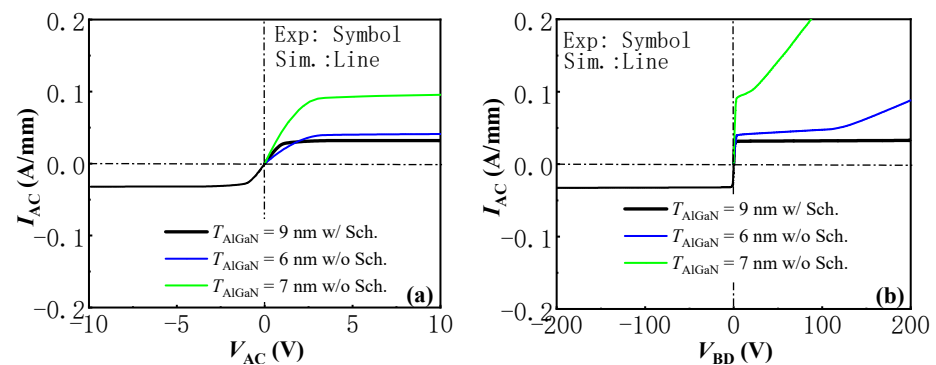


Figure 5. The simulated bidirectional I - V (a) and BV (b) characteristics of the proposed AlGaIn/GaN lateral B-CRD with $L_G = 1 \mu\text{m}$ and $T_{\text{AlGaIn}} = 9 \text{ nm}$, as well as with the simulated I - V and BV characteristics of the bidirectional diode without the Schottky electrode in the recessed structure.

As mentioned, the knee voltage and constant-current density of the proposed AlGaIn/GaN lateral B-CRD were determined by the depth and length of the trench Schottky contact. So, for helping the actual device design, it is necessary to investigate the device characteristic's dependence on the depth and length of the trench Schottky contact. Figure 7 gives the influence of the trench Schottky contact's depth on the bidirectional I - V and BV characteristics of the proposed AlGaIn/GaN lateral B-CRD with $L_G = 1 \mu\text{m}$. It was found that the constant current density of the proposed AlGaIn/GaN lateral B-CRD increased with an increase in T_{AlGaIn} . When T_{AlGaIn} was increased from 9 nm to 12 nm, the constant-current densities increased from 32 mA to 100 mA (an increase of more than 200%). Although the proposed AlGaIn/GaN lateral B-CRD with a large T_{AlGaIn} was able to deliver a higher current density, the pronounced self-heating effect may significantly deteriorate the steadiness of the regulating current as well as the effective operating voltage range, as shown in our pervious experimental results [13]. On the other hand, by reducing T_{AlGaIn} , the gate-to-channel controllability was effectively enhanced due to the smaller gate-to-channel distance, which lead to a much lower knee voltage (the inset in Figure 7) and an improved steadiness in the regulating current. As can also be seen from the figure,

as T_{AlGaN} decreased from 12 nm to 9 nm, the knee voltages decreased from 3 V to 0.6 V. Additionally, the power consumption ($V_K I_{\text{AC}}$) of the proposed AlGaN/GaN lateral B-CRD could be respectably reduced. So, through tailoring the depth of the trench Schottky contact, a desirable knee voltage and constant-current density could be obtained for the proposed AlGaN/GaN lateral B-CRD.

In this part, the influence of the trench Schottky contact length on the bidirectional I - V and BV characteristics of the proposed AlGaN/GaN lateral B-CRD is investigated, as shown in Figure 8. The value of T_{AlGaN} of the trench Schottky contact was set to be 9 nm for the proposed AlGaN/GaN lateral B-CRD. It can be seen that the constant-current densities of the proposed AlGaN/GaN lateral B-CRD increased with a decrease in L_G . As L_G decreased from 1.5 μm to 0.75 μm , the constant-current densities increased from 13 mA to 75 mA. Although the proposed device with a short L_G was able to deliver a higher current density, the device also possessed low breakdown voltage (Figure 8b), which may be due to the short-channel effect. The decrease in the trench Schottky contact length lead to a significant reduction in barrier thickness, which made the electrons more easily transmissible, subsequently reducing the breakdown voltage of the proposed AlGaN/GaN lateral B-CRD. So, to enable the proposed AlGaN/GaN lateral B-CRD with a stable regulating current and a high breakdown voltage, the trench Schottky contact length should be long enough.

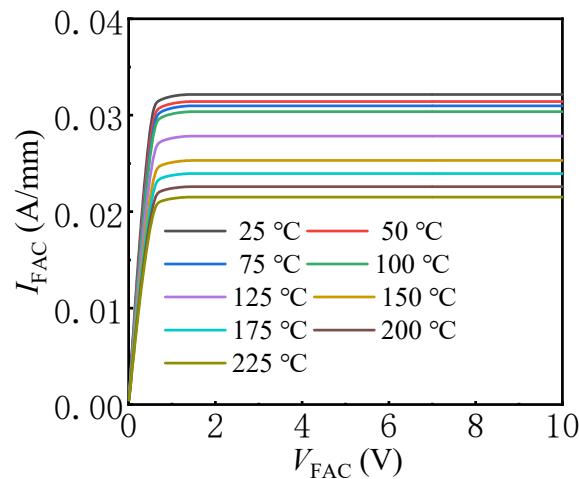


Figure 6. The influence of the temperature on the I - V characteristics of the proposed AlGaN/GaN lateral B-CRD.

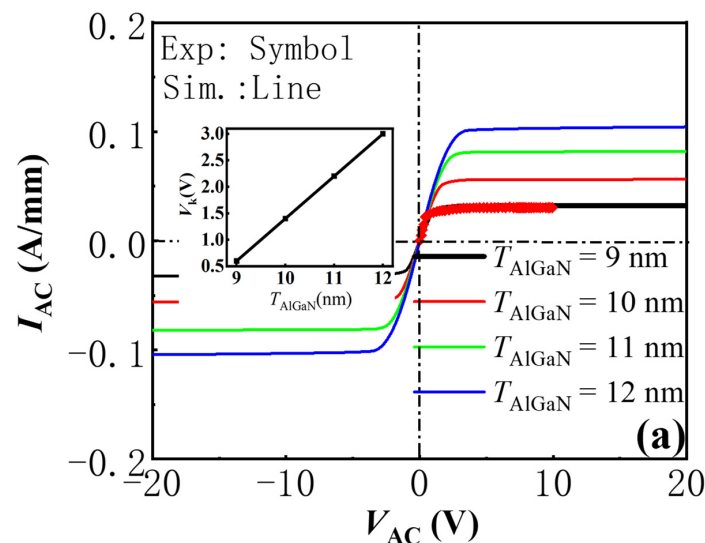


Figure 7. Cont.

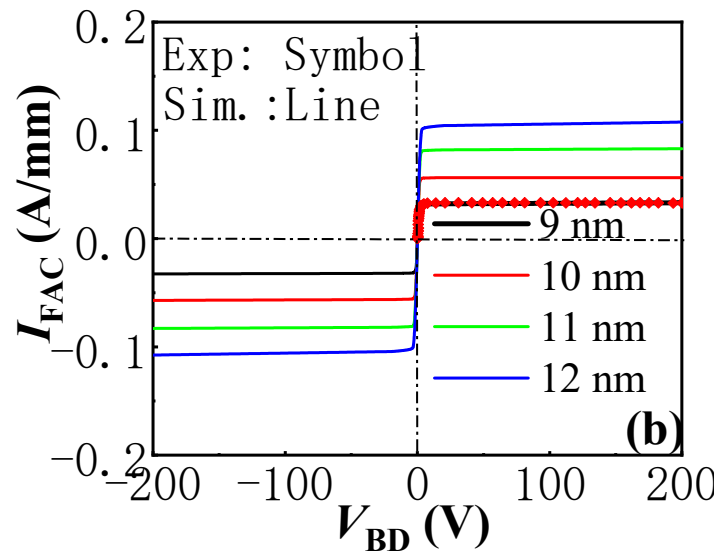


Figure 7. The simulated bidirectional I - V (a) and BV (b) characteristics of the proposed AlGaIn/GaN lateral B-CRD with $L_G = 1 \mu\text{m}$ and different T_{AlGaIn} .

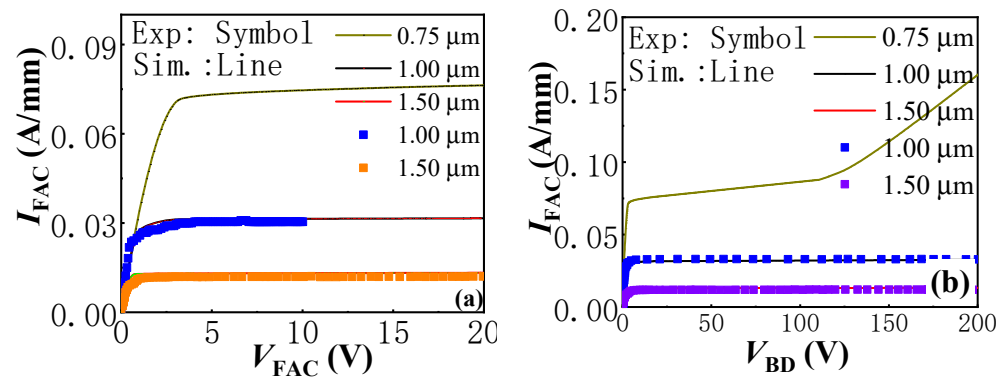


Figure 8. The simulated bidirectional I - V (a) and BV (b) characteristics of the proposed AlGaIn/GaN lateral B-CRD with $T_{\text{AlGaIn}} = 9 \text{ nm}$ and different L_G .

3.2. Switching Characteristics of the Proposed AlGaIn/GaN Lateral B-CRD

Besides outstanding static characteristics, excellent switching characteristics are also important for two-terminal power rectifiers. In this work, the circuit in Figure 1b was employed to evaluate the switching characteristics of the proposed AlGaIn/GaN lateral B-CRD. The depth and length of the trench Schottky contact of the proposed AlGaIn/GaN lateral B-CRD were set to be 9 nm and 1 μm , respectively. As shown above, the proposed AlGaIn/GaN lateral B-CRD with T_{AlGaIn} of 9 nm and L_G of 1 μm possessed a low constant-current density of about 30 mA/mm, even with the applied voltage spanning a range of 0–200 V. In addition, two applied voltages with different directions were employed in this circuit (Figure 9a), which were set to be 100 V and -100 V . In addition, the switching time between the two applied voltages was set to 1 ns.

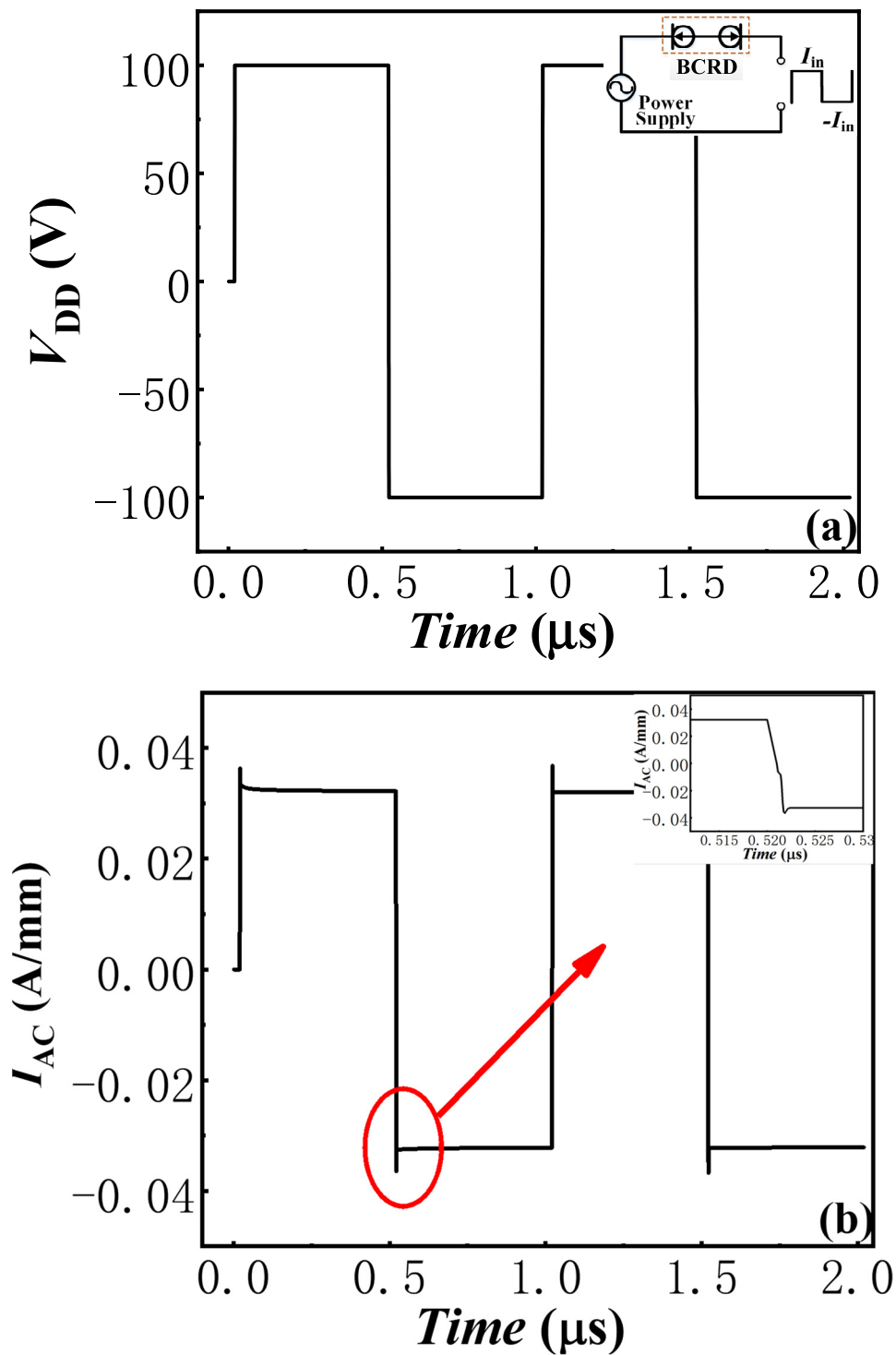


Figure 9. The switching characteristics of the proposed AlGaIn/GaN lateral B-CRD: (a) applied voltage; (b) current.

Figure 9b exhibits the switching characteristics of the proposed AlGaIn/GaN lateral B-CRD. When a high positive voltage of 100 V was applied to the proposed AlGaIn/GaN lateral B-CRD, the device maintained a relatively low and stable forward current of about 30 mA/mm. When the switch was turned to a negative applied voltage, the proposed AlGaIn/GaN lateral B-CRD produced a reverse-current overshoot and a high current change rate, as shown in Figure 9b. The current overshoot may result from the reverse-recovery charge of the hybrid-trench electrodes, just as the reverse-recovery phenomenon

in the AlGa_N/Ga_N lateral-field-effect rectifiers [19]. However, there were very little reverse-recovery charges for the hybrid-trench electrodes. So, the reverse-current overshoot of the proposed AlGa_N/Ga_N lateral B-CRD was very low, and the proposed B-CRD was able to respond quickly to the change in the applied voltage and reached a steady state in a few nanoseconds, even with a very high change rate in the applied voltage. In other words, the proposed AlGa_N/Ga_N lateral B-CRD possessed an excellent switching characteristic. Additionally, the anti-interference ability of the proposed AlGa_N/Ga_N lateral B-CRD was also evaluated by the circuit shown in Figure 1. The applied voltages were set to increase from 50 V to 200 V (Figure 10a), change from 50 V to 60 V or to 40 V (Figure 10b), or change in sine function (Figure 10c). The switching time between the different voltages was also set to 1 ns. Figure 8 exhibits the anti-interference ability of the proposed AlGa_N/Ga_N lateral B-CRD. It was found that the sudden change in the applied voltage had nearly no effect on the current of the proposed AlGa_N/Ga_N lateral B-CRD, demonstrating the proposed B-CRD possessed an excellent anti-interference ability.

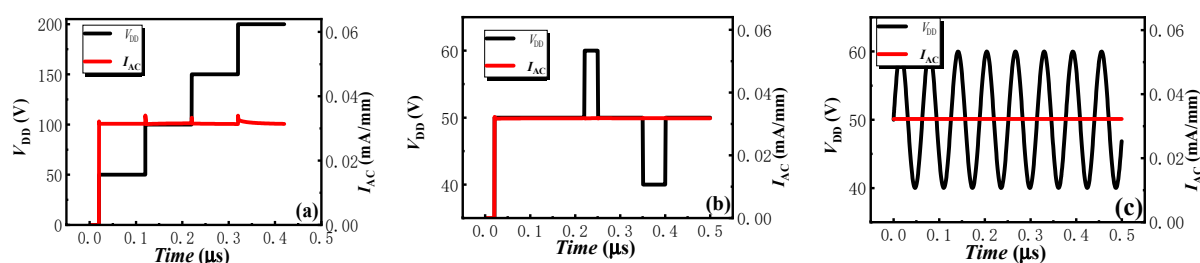


Figure 10. The anti-interference ability of the proposed AlGa_N/Ga_N lateral B-CRD: (a) 50 V to 200 V, (b) change from 50 V to 60 V or to 40 V, (c) change in sine function.

4. Conclusions

A novel AlGa_N/Ga_N lateral B-CRD featuring two symmetrical hybrid-trench electrodes is proposed in this paper. Through the simulation carried out by TCAD Sentaurus, it was demonstrated that the proposed B-CRD was able to deliver an excellent steady current in both directions, even with the applied voltage spanning a large range of 0–200 V. Furthermore, the device's knee voltage and current density showed a strong relation with the depth and length of the trench Schottky contact. Through tailoring the depth and length of the trench Schottky contact, a desirable knee voltage and constant-current density could be obtained for the proposed AlGa_N/Ga_N lateral B-CRD. Additionally, it was also demonstrated through the device/circuit mixed-mode simulation that the proposed B-CRD was able to respond to the change in voltage in a few nanoseconds.

Author Contributions: Conceptualization, Y.S. and Z.C.; methodology, Y.S., Z.C. and Y.H.; validation, Y.S., Z.C., Y.H. and Y.C.; formal analysis, Y.S. and Z.H.; investigation, Y.S. and Z.H.; resources, Y.S. and Z.C.; data curation, Y.S. and Z.H.; writing—original draft preparation, Y.S. and Z.H.; writing—review and editing, Y.S., L.C. and Z.H.; visualization, Y.S. and Z.C.; supervision, G.L. and Y.H.; project administration, Y.S.; funding acquisition, Y.S. and Z.H. All authors have read and agreed to the published version of the manuscript.

Funding: This research was supported by the National Natural Science Foundation of China (NSFC), grant number 62004046, the Key-Area Research and Development Program of Guangdong Province under Grant 2020B010173001, and the Basic scientific research projects in Guangzhou, grant number 202102020317.

Institutional Review Board Statement: Not applicable.

Informed Consent Statement: Not applicable.

Data Availability Statement: Data available on request due to restrictions e.g., privacy or ethical.

Conflicts of Interest: The authors declare no conflict of interest.

References

1. Chen, K.J.; Häberlen, O.; Lidow, A.; Tsai, C.L.; Ueda, T.; Uemoto, Y.; Wu, Y. GaN-on-Si Power Technology: Devices and Applications. *IEEE Trans. Electron Devices* **2017**, *64*, 779–795. [[CrossRef](#)]
2. Shi, Y.; Huang, S.; Bao, Q.; Wang, X.; Wei, K.; Jiang, H.; Li, J.; Zhao, C.; Li, S.; Zhou, Y.; et al. Normally off GaN-on-SiMIS-HEMTs Fabricated with LPCVD-SiNx Passivation and High-Temperature Gate Recess. *IEEE Trans. Electron Devices* **2016**, *63*, 614–619. [[CrossRef](#)]
3. Zhu, M.; Song, B.; Qi, M.; Hu, Z.; Nomoto, K.; Yan, X.; Cao, Y.; Johnson, W.; Kohn, E.; Jena, D.; et al. 1.9-kV AlGaIn/GaN Lateral Schottky Barrier Diodes on Silicon. *IEEE Electron Device Lett.* **2015**, *36*, 375–377. [[CrossRef](#)]
4. Chen, W.; Wong, K.-Y.; Chen, K.J. Single-Chip Boost Converter Using Monolithically Integrated AlGaIn/GaN Lateral Field-Effect Rectifier and Normally off HEMT. *IEEE Electron Device Lett.* **2009**, *30*, 430–432. [[CrossRef](#)]
5. He, Y.; Qiao, M.; Dai, G.; Yu, L.; Zhang, K.; Zhao, X.; Ou, J.; Zhu, X.; Li, Z.; Tang, Y.; et al. A vertical current regulator diode with trench cathode based on double epitaxial layers for LED lighting. In Proceedings of the IEEE 27th International Symposium on Power Semiconductor Devices & IC's (ISPSD), Hong Kong, China, 10–14 May 2015.
6. Current Regulator Diodes, Document 70195, VISHAY, Datasheet. Available online: <https://pdf1.alldatasheet.com/datasheet-pdf/view/84165/LINEAR/J505.html> (accessed on 1 March 2004).
7. Loo, K.H.; Lun, W.K.; Tan, S.C. On driving techniques for LEDs: Toward a Generalized methodology. *IEEE Trans. Power Electron* **2009**, *24*, 2967–2976. [[CrossRef](#)]
8. Hu, Y.; Jovanovic, M.M. LED Driver with Self-Adaptive Drive Voltage. *IEEE Trans. Power Electron.* **2008**, *23*, 3116–3125. [[CrossRef](#)]
9. Kim, J.K.; Lee, J.B.; Moon, G.W. Isolated switch-mode current regulator with integrated two boost LED drivers. *IEEE Trans. Ind. Electron* **2014**, *61*, 4649–4653. [[CrossRef](#)]
10. Zhang, k. *Research and Design of a Vertical Constant Current Diode*; University of Electronic Science and Technology of China: Chengdu, China, 2016; pp. 7–12.
11. Xu, L.; Fan, K.; Sun, H.; Guo, Z. Improving the External Quantum Efficiency of High-Power GaN-Based Flip-Chip LEDs by Using Sidewall Composite Reflective Micro Structure. *Micromachines* **2021**, *12*, 1073. [[CrossRef](#)] [[PubMed](#)]
12. Kim, S.-J.; Oh, S.; Lee, K.-J.; Kim, S.; Kim, K.-K. Improved Performance of GaN-Based Light-Emitting Diodes Grown on Si (111) Substrates with NH₃ Growth Interruption. *Micromachines* **2021**, *12*, 399. [[CrossRef](#)] [[PubMed](#)]
13. Zhang, A.; Zhou, Q.; Shi, Y.; Yang, C.; Shi, Y.; Yang, Y.; Zhu, L.; Chen, W.; Li, Z.; Zhang, B. AlGaIn/GaN Lateral CRDs with Hybrid Trench Cathodes. *IEEE Trans. Electron Devices* **2018**, *65*, 2660. [[CrossRef](#)]
14. Sun, F.; Wang, Y.; Xie, J.; Dou, Q. Research on thermal performance of AC-LED light engine driven by segmented linear constant current driver. In Proceedings of the IEEE 3rd Information Technology and Mechatronics Engineering Conference, Chongqing, China, 3–5 October 2017.
15. Kuo, C.; Liang, T.; Chen, K.; Chen, J. Design and implementation of high frequency AC-LED driver with digital dimming. In Proceedings of the IEEE International Symposium on Circuits and Systems, Paris, France, 30 May–2 June 2010.
16. Qiao, M.; Li, L.; Liang, L.; Song, X.; Zhu, X.; Yu, L.; Zhang, B. LED Constant Current Driving Circuit Having Light Modulation Function. Chinese Patent CN201710311508.7, 5 May 2017.
17. Hwu, K.I.; Tu, W.C. Controllable and Dimmable AC LED Driver Based on FPGA to Achieve High PF and Low THD. *IEEE Trans. Ind. Inform.* **2013**, *9*, 1330–1342. [[CrossRef](#)]
18. Hwu, K.I.; Tu, W.C. A high brightness light-emitting diode driver with power factor and total harmonic distortion improved. In Proceedings of the 26th IEEE Applied Power Electronics Conference and Exposition (APEC), Fort Worth, TX, USA, 6–10 March 2011.
19. Shi, Y.; Chen, W.; Liu, C.; Cui, X.; Li, M.; Xia, Y. Investigation on the Device Geometry-Dependent Reverse Recovery Characteristic of AlGaIn/GaN Lateral Field-Effect Rectifier (L-FER). *Superlattices Microstruct.* **2018**, *120*, 605–610. [[CrossRef](#)]
20. Wang, Z.; Zhang, B.; Chen, W.; Li, Z. A Closed-Form Charge Control Model for the Threshold Voltage of Depletion- and Enhancement-Mode AlGaIn/GaN Devices. *IEEE Trans. Electron Devices* **2013**, *60*, 1607. [[CrossRef](#)]
21. Synopsys, Inc.: Sentaurus Device User Guide. 315–326 in Chapter 12, 344–351 in Chapter 13, 687–690 in Chapter 27 (2010.09). Available online: <https://solvnet.synopsys.com> (accessed on 1 September 2010).